Journal of Alloys and Compounds 696 (2017) 150–154

Contents lists available at ScienceDirect

Journal of Alloys and Compounds

journal homepage: http://www.elsevier.com/locate/jalcom

O-doped Sb materials for improved thermal stability and high-speed phase change memory application

Yifeng Hu [a, *], Xiaoqin Zhu [a, **], Hua Zou [a], Long Zheng [a], Sannian Song [b], Zhitang Song [b]

[a] School of Mathematics and Physics, Jiangsu University of Technology, Changzhou 213001, China
[b] State Key Laboratory of Functional Materials for Informatics, Shanghai Institute of Micro-System and Information Technology, Chinese Academy of Sciences, Shanghai 200050, China

ARTICLE INFO

Article history:
Received 18 September 2016
Received in revised form
12 November 2016
Accepted 19 November 2016
Available online 19 November 2016

Keywords:
Sb material
Oxygen-doping
Thermal stability
High-speed

ABSTRACT

The O-doped Sb materials were proved to have higher crystallization temperature (~205 °C), larger crystallization activation energy (3.95 eV) and better data retention ability (143 °C for 10 years). The band gap was broadened by O-doping and the grain size was refined. The formation of Sb oxide increased the binding energy. The fast phase change speed was obtained for O-doped Sb materials by picosecond laser technology. After O-doping, the phase change film had a smaller surface roughness (1.05 nm).

1. Introduction

As one of the most promising candidates for next-generation non-volatile memory, phase change memory (PCM) has recently attracted much attention due to its high scalability, low power consumption, fast speed, cheap cost and fabrication compatibility with complementary metal-oxide-semiconductor (CMOS) process [1,2]. Under the action of different current pulses, the data storage could be achieved by exploiting a reversible phase change between RESET state (high-resistive amorphous state) and SET state (low-resistive crystalline).

$Ge_2Sb_2Te_5$ (GST) was currently the most widely adopted phase change material which had shown excellent performance [3]. However, Te atoms in GST film could easily segregate to the interface between phase change material and heating electrode due to their high mobility and low melting temperature [4]. The segregated Te element might deteriorate the CMOS manufacturing process and minish the fatigue property. Besides, it was reported that the GST-based PCM devices were difficult to have integrated SET and RESET processes when the electric pulse width was shorter than 100 ns [5]. Recently, Te-free Sb-rich phase change materials have been demonstrated to have fast crystallization rate and good amorphous thermal stability, such as binary GeSb [6,7], SiSb [8], SnSb [9] and ZnSb [10]. Meanwhile, the doping has been applied to improve the thermal property of phase change materials effectively [11,12].

In this paper, O-doped Sb material (SbO*x*) was proposed and systematically studied by resistance versus temperature (*R*–*T*), X-ray diffraction (XRD) and surface topography measurements. The effect of O-doping on the thermal stability, crystallization characteristics, and optical transition of SbO*x* phase-change material were analyzed.

2. Experimental

Undoped and O-doped Sb material with a thickness of 50 nm were deposited on SiO_2/Si (100) substrates by radio-frequency (RF) magnetron sputtering using a single metal target of Sb(99.999%). Oxygen gas was introduced during argon spurting in order to deposit O-doped Sb films. The O concentration was controlled by adjusting the oxygen flow rate with the total gas flow rate fixed at 30 sccm (sccm denotes standard cubic centimeter per minute at STP). The Sb and SbO*x* ($x = 1, 2, 3, 4$) films stood for undoped and O-doped Sb films, respectively. The O concentrations of SbO1, SbO2, SbO3 and SbO4 films, measured by X-ray photoelectron spectroscopy (XPS), were 10.3, 16.7, 21.2 and 25.2 at.%, respectively.

* Corresponding author.
** Corresponding author.
E-mail addresses: hyf@jsut.edu.cn (Y. Hu), pcram@jsut.edu.cn (X. Zhu).

http://dx.doi.org/10.1016/j.jallcom.2016.11.244
0925-8388/

The amorphous-to-crystalline transition was investigated by *in situ* film resistance measurements under an Ar atmosphere. The sample temperature was measured by a Pt-100 thermocouple located at a heating stage controlled by a TP 94 temperature controller (Linkam Scientific Instruments Ltd., Surrey, UK). The phase structures of the films annealed at various temperatures were examined by XRD analyses using Cu Karadiation in the 2θ range from 20° to 60°, with a scanning step of 0.01°. A picosecond laser pump-probe system was used for real-time reflectivity measurement. The light source used for irradiating the samples was a frequency-doubled model-locked neodymium yttrium aluminum garnet laser operating at 532 nm wave-length with a pulse duration of 30 ps? The surface roughness of the film was evaluated by atomic force microscopy (AFM, FM-Nanoview 1000), which was carried out in the semi-contact mode.

3. Results and discussion

Fig. 1a depicted the resistances as a function of temperature for pure Sb and O-doped Sb thin films. With the increase of temperature at a fixed heating rate of 10 °C/min, the resistances of all the O-doped Sb thin films decreased slowly, presenting a semiconductor-like behavior [13]. The temperature at which the amorphous resistance began to decrease sharply was defined as the crystallization temperature T_c. Fig. 1a showed that the T_c for SbO1, SbO2, SbO3 and SbO4 thin films were 165, 185, 195 and 205 °C, respectively. By contrast, pure Sb thin film didn't appear obvious resistance change during heating process. Generally, the thermal stability of amorphous film could be roughly evaluated through the crystallization temperature T_c [5,14]. Therefore, O-doping enhanced the thermal stability of pure Sb thin films. In order to confirm the crystallization state, the subsequent cooling process at the same rate was carried out. Fig. 1a showed the resistances maintained in the low values, indicating the happening of amorphous-to-crystalline phase change. Besides, the resistances of amorphous and crystallization states increased after O-doping, which was helpful for reducing RESET current according to the joule heating equation: $Q = I^2 \cdot R \cdot t$, where Q, I, R, and t were the thermal energy, current, electrical resistance, and time, respectively [15]. Therefore, the programming current was inversely proportional to the resistance of the crystalline phase when fixed thermal energy was employed for melting.

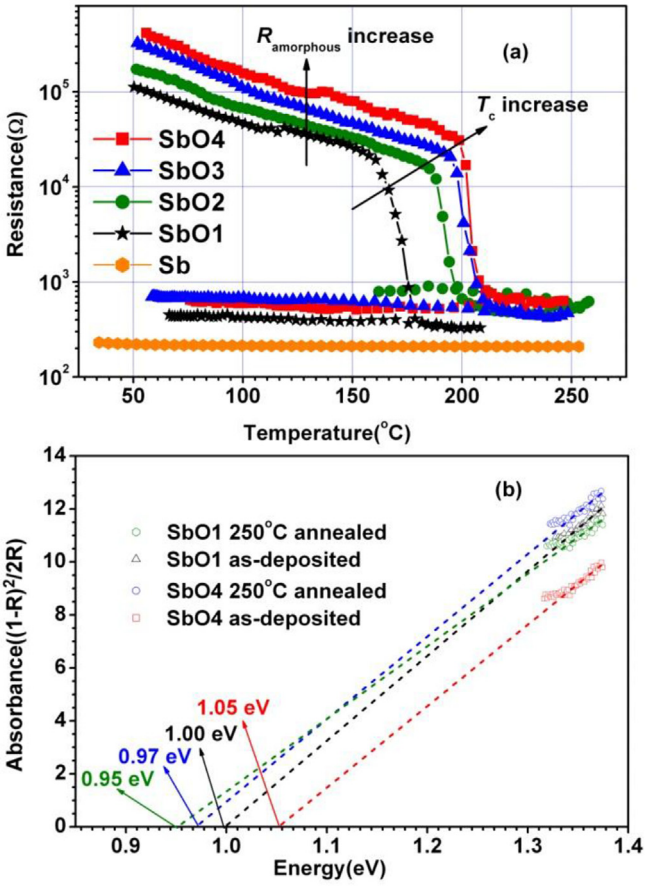

Fig. 1. (a) *R-T* curves of undoped and O-doped Sb thin films; (b)The Kubelka-Munk function of O-doped Sb thin films.

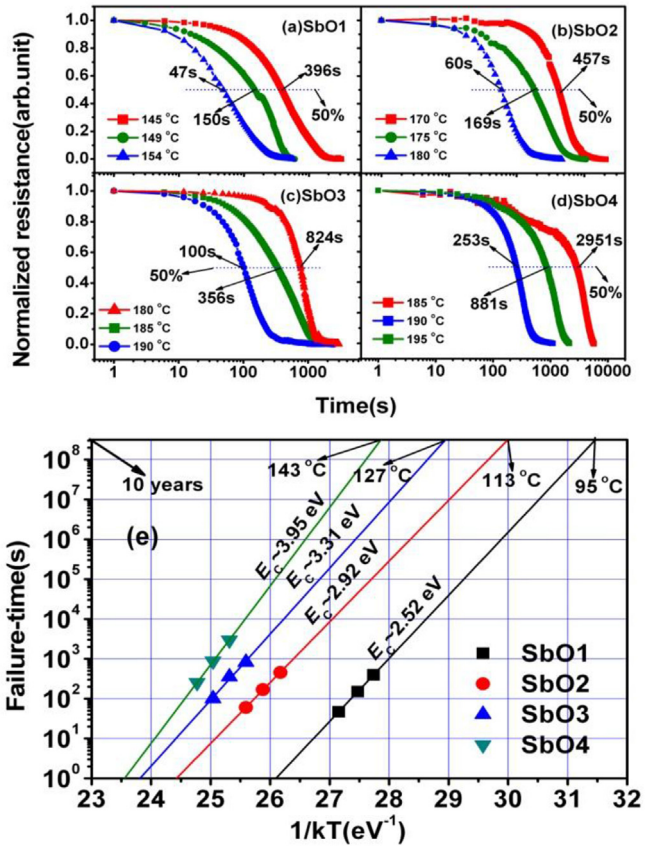

Fig. 2. (a–d) The change of normalized resistance with time for O-doped Sb thin films at isothermal annealing process; (e) Arrhenius plots of failure time vs. 1/kT of O-doped Sb thin films and the extrapolated data retention time at specified temperatures.

The diffuse reflectivity spectra of O-doped Sb thin films before and after crystallization were measured by UV–visible–NIR spectrophotometry in the wavelength range from 200 to 2500 nm. The band gap energy (E_g) could be determined by extrapolating the absorption edge onto the energy axis, as shown in Fig. 1b. Wherein the conversion of the reflectivity to absorbance data was obtained by the Kubelka-Munk function (K-M) [16]:

$$K/S = (1-R)^2/(2R) \quad (1)$$

Where R, K and S were the reflectivity, absorption coefficient and scattering coefficient, respectively. For SbO1 thin film, the E_g decreased from 1.00 eV of as-deposited state to 0.95 eV of 250 °C annealed state. Similarly, the E_g of SbO4 thin film decreased from 1.05 to 0.97 eV after crystallization. Generally, a large optical band gap indicated decreasing electrical conductivity and increasing

resistance because the electrons couldn't move easily from the valence band to the conduction band. Thus, the activation energy for electrical conductivity increased. In addition, the E_g increased with more O-doping. This finding was supported by the change trends of resistance curves in Fig. 1a.

In order to evaluate the data retention of phase change materials, the isothermal crystallization was employed in time-dependent resistance at different temperatures. The change of normalized resistance with time for O-doped Sb thin films at isothermal annealing process was showed in Fig. 2a–d. The failure time was defined as the time when the resistance reached half of its initial value at a specific isothermal temperature. The typical inverse *S*-shaped growth curves could be seen for the isothermal crystallization, including incubation period, steady-state nucleation, growth, and coarsening [17]. For every sample, three isothermal temperatures were selected lower than the T_c. Fig. 2a showed that the failure time of SbO1 thin film at the annealing temperature 154 °C is 47 s. Corresponding to lower annealing temperature 149 and 145 °C, the failure time increased to 150 and 396 s, respectively. A lower isothermal temperature would result in a longer failure time because it needed more time to accumulate the energy for the nucleation and grain growth. The similar change trends could be obtained for SbO2, SbO3 and SbO4 films. What's more, the failure time for 185 °C annealed SbO4 film was 2951 s, which was much longer than that of 145 °C annealed SbO1 film (396 s). Thus, the data retention was greatly improved by O doping.

The plot of logarithm failure time vs. $1/(k_bT)$, which fitted a linear Arrhenius relationship due to its thermal activation nature, could be described as [18].

$$t = \tau_0 \exp[E_c/(k_b \times T)] \quad (2)$$

where t, τ_0, k_b, and T were failure time, the pre-exponential factor depending on the material's properties, Boltzmann's constant and absolute temperature of concern, respectively. The activation energy E_c of SbO1 thin film obtained from the slope of Fig. 2e was 2.52 eV. With increase of oxygen content, E_c of O-doped Sb thin films increased from 2.92 of SbO2 to 3.95 eV of SbO4. Accordingly, the 10-year retention temperatures for SbO1, SbO2, SbO3 and SbO4 thin films were 95, 113, 127 and 143 °C, respectively. From this perspective, O-doped Sb thin films possessed better reliability of the resistance state to meet the application of data storage at elevated temperature.

The XRD patterns of pure Sb and SbO4 materials annealed at different temperatures were shown in Fig. 3a and b, respectively. In as-deposited pure Sb material, a weak diffraction peak (110) at 42.5° of Sb phase could be seen, indicating some Sb grains have formed during deposition process due to poor thermal stability of Sb material. With increase of annealing temperature, no new diffraction peaks were observed and the peak (110) became stronger, which was in accord with the result of Fig. 1a. Being different from pure Sb, no diffraction peaks existed in as-deposited and 150 °C annealed SbO4 materials in Fig. 3b. After annealing at 200 °C for 10 min, the characteristic peak (110) appeared, belonging to Sb phase. Then, a new diffraction peak of Sb_2O_3 (440) was observed in 230 and 250 °C annealed SbO4 materials, indicating new phase has formed after O doping. From the main peak at

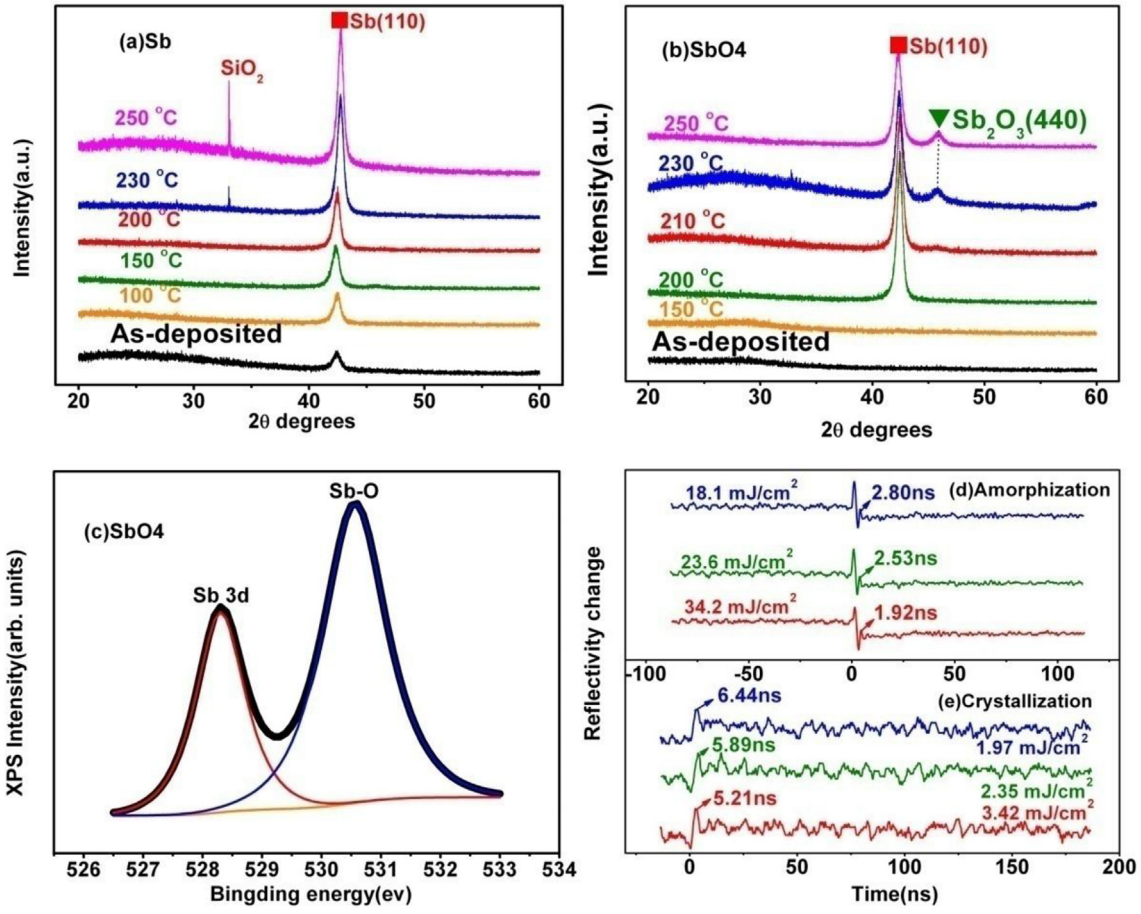

Fig. 3. XRD patterns of (a) Sb, (b) SbO4 thin films annealed at different temperatures for 10 min in Ar atmosphere; (c) XPS spectra of SbO4 thin film for Sb 3d; Reversible reflectivity evolution of SbO4 thin films induced by consecutive picosecond laser pulses with different fluences: (d) amorphization process (e) crystallization process.

around 42.5° with the same annealing temperature 250 °C, the grain sizes of annealed Sb and SbO4 films were 25.6 and 16.3 nm, respectively, calculated using the Scherrer equation ($D_{hkl} = 0.943\lambda/\beta cos\theta$). The decreased grain size could produce more grain boundaries, which helped to enhance the electron scattering, thus leading to a higher resistance [19]. This result interpreted the resistance increasing of O-doped Sb film from the structural aspect.

XPS measurement of SbO4 thin film was performed to further study the effect of oxygen doping on the changes of chemical bonding state of elements. Fig. 3c showed the XPS spectra of Sb 3d for SbO4 films. Two peaks at 528.30 eV and 530.80 eV could be seen in the XPS spectra of Sb 3d [20]. The binding energy at 528.30 eV could be assigned to a typical binding energy for the bond of Sb–Sb. While for the energy of 530.80 eV, close matches were found with the binding energy of Sb $3d_{5/2}$ for the bond of Sb–O. The consensus finding has been obtained in XRD analysis. The electronegativity of Sb and O elements was 1.8 and 3.5, respectively [15]. That was, Sb atom had higher affinity with O atom than Sb atom, which would result in the increase of binding energy of Sb 3d. Due to the adding of oxygen atoms, some Sb atoms in Sb–Sb bonds have been replaced by oxygen atoms to form Sb–O oxides. The Sb–O oxides condensed near grain boundaries and wrapped around the crystal grains [21]. The atomic migration could be suppressed, resulting in smaller grain size and larger number of grain boundaries [5].

The phase change was accompanied by the changes of electrical resistivity as well as optical reflectivity [22]. The picosecond laser technology was used to investigate the switching speed of phase change materials. In Fig. 3d, the reflectivity dropped, indicating the crystalline-to-amorphous state transition. Corresponding to different irradiation fluences of 18.1, 23.6 and 34.2 mJ/cm^2, the amorphization time were 2.80, 2.53 and 1.92 ns, respectively. That was, a larger irradiation fluence would result in a shorter phase change time. Fig. 3e showed that a converse phase transform was achieved with an abrupt increase of optical reflectivity. Thus, a reversible phase change could be realized with laser pulses. The crystallization time was used as the valuation criteria of phase-change speed because the crystallization process needed more time than the amorphization one [23]. With the irradiation fluences of 1.97, 2.35 and 3.42 mJ/cm^2, the crystallization time were 6.44, 5.89 and 5.21 ns, respectively. It was reported that the crystallization time of GST was 39 ns induced by a laser irradiation fluence of 11.59 mJ/cm^2 [16]. Therefore, SbO4 thin film had a faster switching speed. As was known, Sb-rich phase-change materials had a growth-dominated crystallization behavior rather than a nucleation-dominated one [24]. As demonstrated by the XPS spectra (Fig. 3c), the excess Sb formed weak Sb-Sb bonds in SbO4 thin film. In the crystallization process, the dispersed Sb-Sb bonds were easily broken and could act as heterogeneous nucleating agents. This provided a large number of starting positions for crystallization and accelerated the phase change of the material [25].

In phase change process, the internal stress of materials would result in the change of surface properties. For PCM, film surface roughness had a significant impact on device performance because it would affect the quality of the electrode-film interface [26]. The AFM images of Sb and SbO4 thin films before and after crystallization were presented in Fig. 4. The surfaces of as-deposited Sb and SbO4 thin films were very smooth, with the root-mean-square surface roughness 1.27 nm for Sb and 0.35 nm for SbO4 thin films. After annealing at 250 °C for 10 min, the roughness of Sb film increased to 7.85 nm due to the grain growth. In contrast, the roughness of annealed SbO4 film increased slightly to 1.03 nm. This

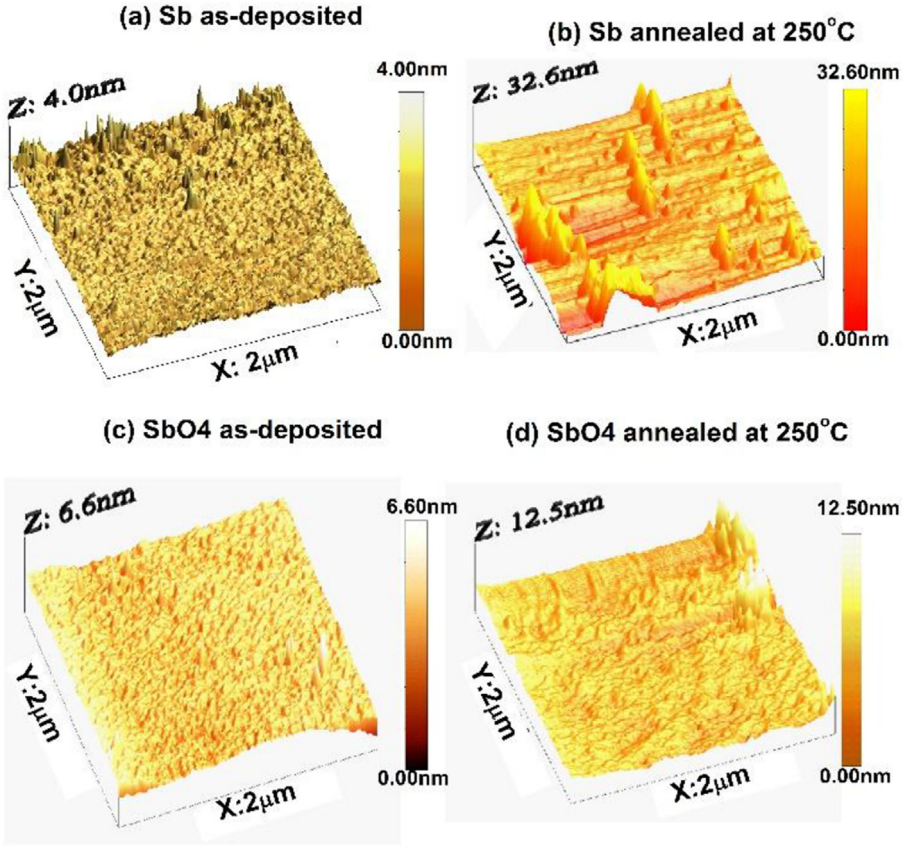

Fig. 4. AFM topographic images of (a) as-deposited Sb, (b) annealed Sb at 250 °C, (c) as-deposited SbO4,(d) annealed SbO4 at 250 °C.

showed that O-doping reduced the grain growth rate, resulting in smaller grain size and stress change.

4. Conclusions

In summary, O-doped Sb materials were investigated for the potential application in PCM. O-doping improved the amorphous thermal stability of Sb materials (SbO2: T_c 185 °C, E_a 2.92 eV; SbO3: T_c 195 °C, E_a 3.31 eV; SbO4: T_c 200 °C, E_a 3.95 eV). The $T_{10\text{-year}}$ of O-doped Sb materials (SbO3: 127 °C; SbO4: 143 °C) were higher than that of GST. More O-doping resulted that the band-gap widths were extended. The crystallization was restrained due to oxygen adding and new Sb oxide phase formed. Some of Sb atoms in Sb-Sb bonds were replaced by oxygen atoms to form Sb-O bonds, resulting in larger binding energy. The crystallization time for SbO4 material induced by picosecond laser pulse was much less than that of GST. In O-doped Sb materials, the surface roughness became smaller (SbO4: 1.03 nm). These results demonstrated that the O-doped Sb material was a promising candidate for high stability and high-speed PCM applications.

Acknowledgments

This work was supported by Natural Science Foundation of Jiangsu Province (BK2015020024) and Changzhou Science and Technology Bureau (No. CJ20160028 and CJ20159049) and Basic Research Program of Jiangsu Education Department (No. 15KJB430012 and 16KJB140004) and Open Fund of State Key Laboratory of Functional Materials for Informatics (KYZ14031) and sponsored by Qing Lan Project.

References

[1] X.Q. Zhu, Y.F. Hu, H. Zou, J.H. Zhang, Y.M. Sun, W.H. Wu, L. Yuan, L.J. Zhai, S.N. Song, Z.T. Song, Scr. Mater. 121 (2016) 66.
[2] Y.H. Zheng, Y. Cheng, M. Zhu, X.L. Ji, Q. Wang, S.N. Song, Z.T. Song, W.L. Liu, S.L. Feng, Appl. Phys. Lett. 108 (2016).
[3] Y.F. Hu, H. Zou, J.H. Zhang, J.Z. Xue, Y.X. Sui, W.H. Wu, L. Yuan, X.Q. Zhu, S.N. Song, Z.T. Song, Appl. Phys. Lett. 107 (2015) 263105.
[4] Y. Zhang, J. Feng, B.C. Cai, Semicond. Sci. Tech. 24 (2009) 045016.
[5] Y.G. Lu, S.N. Song, X. Shen, Z.T. Song, G.X. Wang, S.X. Dai, Thin Solid Films 589 (2015) 215.
[6] H.Y. Cheng, S. Raoux, J.L. Jordan-Sweet, J. Appl. Phys. 115 (2014) 093101.
[7] Y.G. Lu, S.N. Song, X. Shen, L.C. Wu, Z.T. Song, B. Liu, S. Dai, Q.H. Nie, ECS Solid State Lett. 2 (2013) 94.
[8] H. Huang, S.M. Li, F.X. Zhai, Y. Wang, T.S. Lai, Y.Q. Wu, F.X. Gan, Mater. Chem. Phys. 128 (2011) 405.
[9] Y.F. Hu, J.W. Zhai, H.R. Zeng, S.N. Song, Z.T. Song, J. Appl. Phys. 117 (2015) 175704.
[10] G.X. Wang, X. Shen, Y.G. Lu, S.X. Dai, Q.H. Nie, T.F. Xu, J. Alloy. Compd. 622 (2015) 341.
[11] Y.F. Hu, X.Q. Zhu, H. Zou, Y. Lu, J.Z. Xue, Y.X. Sui, W.H. Wu, L. Yuan, S.N. Song, Z.T. Song, J. Mater. Sci. Mater. El 26 (2015) 7757.
[12] X.Q. Zhu, Y.F. Hu, J.Z. Xue, Y.X. Sui, W.W.H.L. Zheng, L. Yuan, S.N. Song, Z.T. Song, S.P. Sun, J. Mater. Sci. Mater. El 25 (2014) 2943.
[13] Y.F. Hu, X.Q. Zhu, H. Zou, J.H. Zhang, L. Yuan, J.Z. Xue, Y.X. Sui, W.H. Wu, S.N. Song, Z.T. Song, Appl. Phys. Lett. 108 (2016) 223103.
[14] Y.G. Lu, S.N. Song, X. Shen, G.X. Wang, L.C. Wu, Z.T. Song, B. Liu, S.X. Dai, J. Alloys Compd. 586 (2014) 669.
[15] J.H. Park, J.H. Jeong, D.J. Choi, Phys. Status Solidi A 213 (2016) 1526.
[16] X.Q. Zhu, Y.F. Hu, L. Yuan, Y.X. Sui, J.Z. Xue, D.H. Shen, J.H. Zhang, S.N. Song, Z.T. Song, J. Electron. Mater. 44 (2015) 3322.
[17] Y.G. Lu, S.N. Song, X. Shen, Z.T. Song, L.C. Wu, G.X. Wang, S.X. Dai, Appl. Phys. A-Mater. Sci. Process 117 (2014) 1933.
[18] Y.F. Hu, Z.F. He, J.W. Zhai, P.Z. Wu, T.S. Lai, S.N. Song, Z.T. Song, Appl. Phys. A-Mater. 121 (2015) 1125.
[19] W.H. Wu, Y.F. Hu, X.Q. Zhu, Y.X. Sui, L. Yuan, L. Zheng, H. Zou, Y.M. Sun, S.N. Song, Z.T. Song, J. Mater. Sci. Mater. El 27 (2016) 2183.
[20] Y.F. Hu, M.C. Sun, S.N. Song, Z.T. Song, J.W. Zhai, J. Alloy. Compd. 551 (2013) 551.
[21] C. Peng, L.C. Wu, F. Rao, Z.T. Song, X.L. Zhou, M. Zhu, B. Liu, D.N. Yao, S.L. Feng, P.X. Yang, J.H. Chu, Scr. Mater. 65 (2011) 327.
[22] Z.Y. Li, Y.F. Hu, T. Wen, J.W. Zhai, T.S. Lai, J. Appl. Phys. 117 (2015) 135703.
[23] C.Q. Zhu, J. Ma, X.M. Ge, F. Rao, K.Y. Ding, S.L. Lv, L.C. Wu, Z.T. Song, Appl. Phys. Lett. 108 (2016) 252102.
[24] X.L. Zhou, L.C. Wu, Z.T. Song, F. Rao, K. Ren, C. Peng, S.N. Song, B. Liu, L. Xu, S.L. Feng, Appl. Phys. Lett. 103 (2013) 072114.
[25] Y.F. Hu, H. Zou, L. Yuan, J.Z. Xue, Y.X. Sui, W.H. Wu, J.H. Zhang, X.Q. Zhu, S.N. Song, Z.T. Song, Scr. Mater. 115 (2016) 19.
[26] T. Zhang, Z.T. Song, F. Wang, B. Liu, S.L. Feng, B.M. Chen, Appl. Phys. Lett. 91 (2007) 221102.